A decentralized FLISR model for resilient smart grids

Chaudhary Talha Hassan, Muhammad Shamaas, Tariq Mahmood Jadoon
Department of Electrical Engineering
Lahore University of Management Sciences
Lahore 54792, Pakistan
chaudhry.hassan@lums.edu.pk, muhammad.shamaas@lums.edu.pk, jadoon@lums.edu.pk

***Abstract*—Resilient smart grids must guarantee fast service restoration of critical loads during unexpected blackouts. This can be achieved by isolating the faults and forming microgrids around black-start generators. A self-sufficient microgrid must ensure optimal control of distributed generators without causing overloads or transient instability. Microgrid dynamic stability must be enforced after every restoration stage by analyzing the power system transient response. In this research, measurements from distributed phasor measurement units are used to quantify the disturbance experienced by the generators in each restoration stage. This feedback is used to modulate the load restoration limit of the next restoration stage. Decentralized control is implemented to solve the serious challenges of information discovery, real-time task scheduling, communication network congestion, and big data analysis. The importance of multi-agent coordination is analyzed by simulating network traffic of control and metering systems. The approach is validated over a modified IEEE-123 node test feeder.**

***Index Terms*--Energy storage system (ESS), inverter-based distributed generator (IBDG), mixed-integer second-order cone programming (MISOCP), wide-area situational awareness (WASA).**

I. Introduction

Modern smart grids must guarantee high reliability of service to consumers. Although faults are inevitable, uninterruptible service must be ensured for critical loads. During an unexpected emergency, the generation capacity and energy reserves must be carefully utilized to recover critical loads. An effective method for emergency service restoration is the sectionalization of the power network into microgrids [1]. These autonomous units coordinate all the decisions for self-healing. Hence, power restoration can be achieved in a decentralized manner [2].

An intelligent control system must be well informed about the situation of all the constituent subsystems. The control commands must be based on real-time data obtained from distributed field devices [2]. In short, an active management system is needed to sense and optimally control all the distributed subsystems. The proposed fault location and service restoration (FLISR) model [3] is shown in Figure 1.

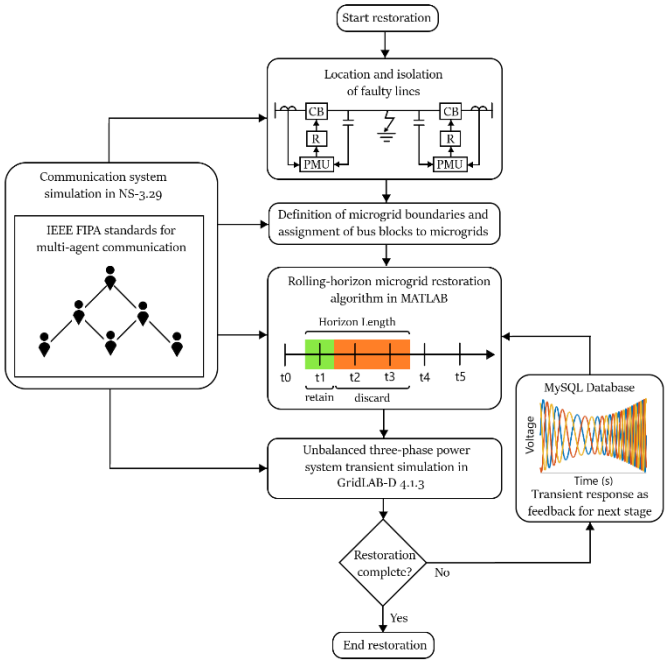

Figure 1: FLISR model for smart grid.

This research aims to achieve the following goals:

1. Develop a decentralized multi-agent system architecture for the restoration of inverter-dominated microgrids [2] [4]. The microgrid restoration was based on the prior information of distributed generators, distribution network configuration, and load demand forecast [2]. The microgrid controller performed MISOCP optimization for demand response, and network reconfiguration. Based on the restoration solution, it distributed control commands to the different smart switches and bus block controllers.

2. Develop a pervasive communication system to coordinate the control and protection of microgrids during sequential service restoration [2] [4] [5]. The microgrid controller was responsible for monitoring all the widespread loads, lines and generators. It aggregated the status information and distributed the control commands for the GridLAB-D simulation [6]. The hierarchical structure for data exchange was implemented using separate control and metering systems in NS-3 [7].

3. Quantify the disturbance experienced during each microgrid restoration stage to provide feedback for the microgrid protection system [1]. After every restoration stage, the transient fault records of the GridLAB-D [6] simulation were collected to quantify the disturbance experienced by the microgrid. The maximum deviations in generator voltages, powers, and frequencies were used to calculate the microgrid disturbance factor. A rolling horizon optimization framework was implemented to modulate the load restoration limit based on the microgrid disturbance factor.

II. Formulation Of Optimization Problem

A MISOCP optimization problem was formulated for the restoration of the damaged IEEE-123 bus system [8] shown in Figure 2. The modified network contained three-phase diesel generators, PV generators, and EV charging stations. Each generator had a rating of 1 MVA and a ramp limit of 150 kW/s.

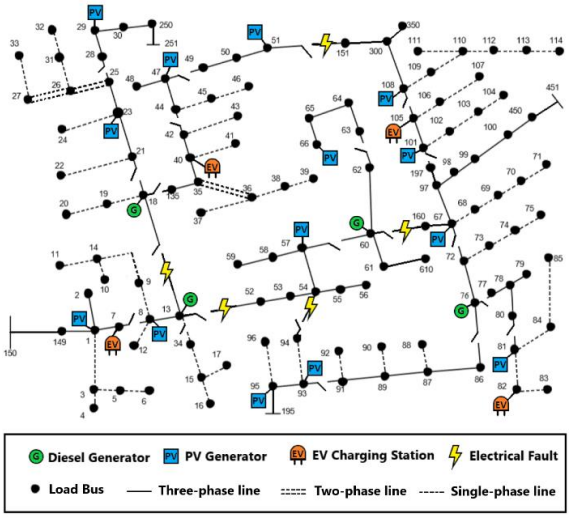

Figure 2: Damaged IEEE 123 bus distribution network.

The service restoration system executed a self-healing algorithm. The initial decision for network reconfiguration was based on the fault location input. The unhealthy region was isolated immediately. Afterward, iterative microgrid formation started. The MISOCP service restoration optimization problem is summarized as follows:

Maximize the sum of restored bus blocks in the time horizon [t, t + T] subject to the following constraints:

1. Nodal active/ reactive power balance constraints: For each node, the total power generation must be equal to the sum of load power, transmitted power and line losses.
2. Nodal voltage constraints: The nodal voltages must be maintained within the desired limits $V^{base} \pm 0.05\ p.u.$
3. Transmission line voltage drop constraints: The voltage drop across an energized transmission line must be greater than or equal to the voltage drop across the transmission line impedance.
4. Transmission line active/ reactive power loss constraints: The line losses must be greater than or equal to the power losses across the series line impedance.
5. Transmission line capacity constraints: The maximum apparent power flow across an energized line must not exceed the line capacity limit.
6. Generator capacity constraints: The apparent power generation of an online generator must be within the generator capacity limits. Also, the power ramp rate limits must not be violated.
7. Battery energy storage system constraints: The battery state of charge must be maintained within the desired limits. An inverter-based generator can absorb or deliver active/ reactive power to control the battery state of charge.
8. Load constraints: Whenever, a switchable line is closed to connect energize a bus block, all of the buses and loads in that bus block must be energized.
9. Radial network constraints: Microgrid restoration must begin by starting a diesel generator with black-start capability. The switchable lines and bus blocks must be energized carefully to maintain radial network topology. A switchable line cannot be energized if the bus blocks of both ends are already energized. Also, a bus block can be energized by only one of the connected switchable lines.
10. Dynamic constraints: After a restoration stage was executed, the maximum values of frequency deviation $\Delta f_{g,t}^{meas}$, apparent power deviation $\Delta S_{g,\varphi,t}^{meas}$, and voltage deviation $\Delta V_{g,\varphi,t}^{meas}$ were recorded for each generator g. These values were translated into the microgrid disturbance factor $DF_{m,t}$ given in (1). This factor was used to modulate the limit of additional load restored in the next stage $\Delta P_{m,t+1}^{res}$, as expressed in (2)-(3). α is the hyper-parameter for calculating the load restoration limit $P_{m,t+1}^{res}$. The base frequency, base voltage and base power was f^{base}, V^{base} and S^{base} respectively.

$$DF_{m,t} = \frac{1}{7}\left[\sum_{g\epsilon\Omega_m}\frac{1}{N_i}\left(\frac{\Delta f_{g,t}^{meas}}{f^{base}} + \frac{\Delta V_{g,\varphi_A,t}^{meas}+\Delta V_{g,\varphi_B,t}^{meas}+\Delta V_{g,\varphi_C,t}^{meas}}{V^{base}} + \frac{\Delta S_{g,\varphi_A,t}^{meas}+\Delta S_{g,\varphi_B,t}^{meas}+\Delta S_{g,\varphi_C,t}^{meas}}{S^{base}}\right)\right] \quad (1)$$

$$\forall m \forall t \epsilon [1,\infty)[\Delta P_{m,t+1}^{res} = \Delta P_{m,t}^{res} + \alpha(1 - DF_{m,t})] \quad (2)$$

$$\forall m \forall t \epsilon [1,\infty)[0 \le P_{m,t+1}^{res} \le P_{m,t}^{res} + \Delta P_{m,t+1}^{res}] \quad (3)$$

III. Multi-agent Coordination Model

The implementation of the optimal power flow solution can present serious challenges during information discovery, real-time task scheduling, communication network congestion and big data analysis [3] [4]. Perfect coordination must be maintained between the microgrid controller, distributed generators and smart switches to prevent microgrid instability [1].

The distributed control system has to schedule multiple hard real time tasks for execution of the optimal solution. It

must also ensure that each real time task has reasonable delay, duration and deadline constraints. Centralized control is not a viable option for this safety-critical system [4]. A multi-agent control scheme was developed to facilitate control and monitoring of the wide area network [3] [2]. The complete multi-agent system for a microgrid team is shown in Figure 3. Each microgrid was divided into several bus block teams headed by bus block master agents. Switch agents were responsible for connecting bus blocks together. Switch agents and bus block agents were controlled by the microgrid controller [5] [6].

IEEE FIPA standard was used to build a unified model for the communication of reactive agents. Agent Communication Language (ACL) was used to transmit information signals between agents [5] [6].

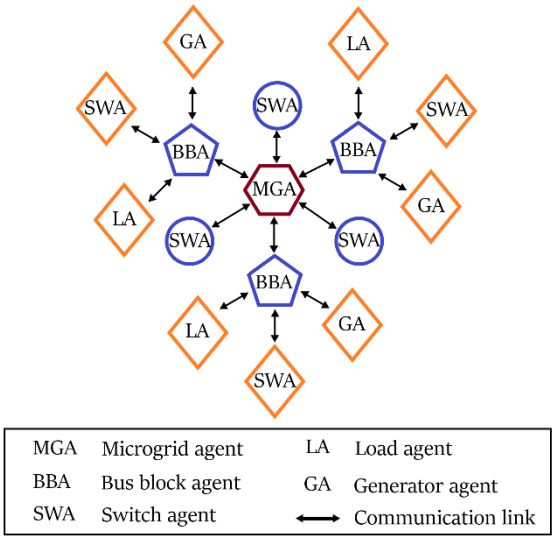

Figure 3: Multi-agent system for a microgrid.

A three-level communication network was designed in NS-3 to enable the coordination between the microgrid controllers and bus block controllers [7]. Control signals were transmitted through the control system, whereas the metering data was transmitted through the monitoring system. Intelligent Electronic Devices (IEDs) installed in the field provided feedback for the reliable control of distributed generators, loads and smart switches [6] [2]. The complete communication system is shown in Figure 4.

A. *Monitoring System*

The AMI system was made up of smart meters, communication modules, data concentrators, and Meter Data Management System (MDMS). MDMS managed data storage to provide the information in a useful form to the microgrid controller. The IEEE C37.118 synchronized phasor measurement units (PMUs) reported the magnitude and phase angle of electrical voltage and current using a common time source for synchronization.

The Wide Area Network (WAN) provided remote access of bus blocks to the microgrid controller via long-range, high-capacity WiMAX links. NS-3 provided a realistic implementation of the IEEE-802.16 standard using wireless MAN-OFDM physical layer, uplink and downlink schedulers, IP packet classifier for the convergence sub-layer, and support for multicast traffic [7]. A base station was installed to serve the subscriber stations installed at the microgrid controller and the bus block controller nodes. The point-to-multipoint telecommunication network enabled pervasive control of the entire distribution system for time-sensitive tasks like maintaining electrical stability [4].

Existing power lines were used to transmit control and status signals across the Field Area Network (FAN). 2 Mbps links were used for power line carrier communication [7]. Each power line communication device was supplemented with a data concentrator for communication with the widespread IEDs [6] [3]. Distributed generators were controlled via programmable logic controllers integrated with SCADA modems. The transmission line channels also conveyed switching commands for capacitor banks, load controllers, and circuit breakers.

The Home Area Network (HAN) connected load controllers and sensors via an Ethernet-based AMI. This enabled coordination of a large number of distributed IEDs [4]. These devices continuously collected information from power meters, transducers, and field components for supervision. 100 Mbps Ethernet links were installed for the Home Area Network. For fast and reliable communication, the IPv4 protocol was implemented in the network layer, and the UDP protocol was implemented in the transport layer [3] [6] [7]. The network interface module implemented distributed network protocols for physical interface conversion. The pervasive communication system enabled continuous scanning of operational data for greater control and flexibility.

B. *Control System*

The microgrid controller distributed command signals using high priority control packets. It was crucial to transmit control signals reliably with very low latency [3]. Control signal channels were designed to have low bandwidth but very high reliability (> 99 %). The maximum constraint for control packet latency was 20 ms.

The priority associated with a socket was used to determine the value of the Differentiated Services field (RFC 2474) of the IPv4 header. This is how DSCP values mapped onto priority values of the packets sent through that socket. DSCP CS6 (RFC 4594) was assigned for high priority network control packets. The packet priority was used by queueing disciplines to classify packets into distinct FIFO queues [7].

The microgrid agent was connected to the bus block agents using wireless LTE links in NS-3. The microgrid controller was connected to bus block UE through eNB, SGW and PGW nodes. The 3GPP specified S5 protocol stack, S1-U protocol stack and LTE radio protocol stack were simulated in LTE-EPC data plane. S1-MME, S11, S5 and X2 interface was modeled for the LTE-EPC control plane [7].

OpenFlow switch was installed in each bus block to connect bus block agent with the generator, switch and load

agents. OpenFlow switch provides the programmability and flexibility required for smart grid architectures with ever-increasing demand [4]. It provides support for traffic engineering and virtual private networks. These features are vital to enhance the reliability and scalability of the smart grid [7].

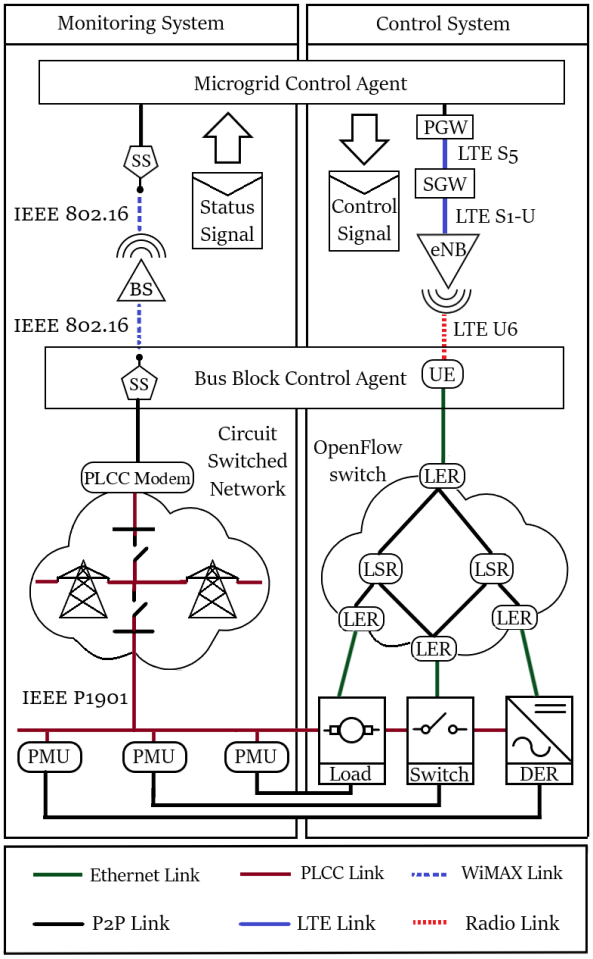

Figure 4: Communication system for monitoring and control signals.

IV. Simulation Results

The simulation of the cyber-physical smart grid was carried out in three steps. First, the MISOCP optimization problem was solved to determine the optimal switching and control commands. Then, the NS-3 communication system simulation was run to determine the delays in the transmission of information to different subsystems. Finally, the outputs from the previous two simulations were implemented in the GridLAB-D simulator to determine the power system transient response [6].

The frequency of grid-forming diesel generators is shown in Figure 5. The restoration of microgrid 1 completed in three stages and involved 1128 messages. The timeline of the three stages of restoration is given below:

1. IBDG 8 ramped up to 815.4 kW. At 0.776 s, bus block 2 was energized by closing the circuit breakers of diesel generator 13 and IBDG 8.
2. IBDG 1, 7 and 8 were ramped up to 245.5 kW, 243.5 kW and 617.4 kW respectively. At 2.414 s, bus block 1 was energized by closing the circuit breaker of line 7-8.
3. IBDG 1, 7 and 8 were ramped up to 342.6 kW, 346.9 kW and 577.0 kW respectively. At 3.585 s, circuit breaker of line 13-34 was closed to energize bus block 3.

The restoration of microgrid 2 completed in four stages and involved 2658 messages. The timeline of the four stages of restoration is given below:

1. IBDG 23 and 40 ramped up to 604.8 kW and 858.6 kW respectively. Bus blocks 4, 5 and 7 were energized at 0.326 s, 1.630 s and 2.712 s respectively.
2. IBDG 23, 29 and 40 ramped up to 659.2 kW, 119.9 kW and 669.4 kW respectively. At 5.116 s, bus block 6 was energized by closing circuit breaker of line 25-28.
3. IBDG 23, 29, 40 and 47 ramped up to 633.9 kW, 249.6 kW, 715.7 kW and 138.4 kW respectively. At 6.153 s, bus block 8 was energized by closing circuit breaker of line 42-44.
4. IBDG 23, 29, 40, 47 and 51 ramped up to 636.8 kW, 356.5 kW, 729.0 kW, 281.6 kW and 131.2 kW. At 7.153 s, bus block 9 was energized by closing the circuit breaker of line 47-49.

The restoration of microgrid 3 completed in three stages and involved 888 messages. The timeline of the three stages of restoration is given below:

1. At 0.306 s, bus block 11 was energized by closing the circuit breaker of diesel generator 60.
2. IBDG 57 ramped up to 88.6 kW. At 1.548 s, bus block 10 was energized by closing the circuit breaker of line 57-60.
3. IBDG 57 and 66 ramped up to 199.1 kW and 123.7 kW respectively. At 2.833 s, bus block 10 was energized by closing the circuit breaker of line 62-63.

The restoration of microgrid 4 completed in four stages and involved 3048 messages. The timeline of the four stages of restoration is given below:

1. At 0.571 s, bus block 14 was energized by closing the circuit breaker of diesel generator 76. At 1.041 s, bus block 15 was energized by closing the circuit breaker of line 76-77.
2. At 3.112 s, bus block 13 was energized by closing the circuit breaker of line 67-72.
3. IBDG 67, 81, 82, 101 and 105 ramped up to 175.9 kW, 109.5 kW, 107.5 kW, 91.3 kW and 90.0 kW respectively. Bus blocks 16, 17 and 19 were energized at 4.676 s, 5.532 s and 6.612 s respectively.
4. IBDG 67, 81, 82, 93, 95, 101 and 105 ramped up to 197.5 kW, 263.3 kW, 249.5 kW, 128.9 kW, 123.9 kW, 176.3 kW and 189.9 kW respectively. At 8.935 s, bus block 18 was energized by closing the circuit breaker of line 91-93. At 10.156 s, bus block 20 was energized by closing the circuit breaker of line 105-108.

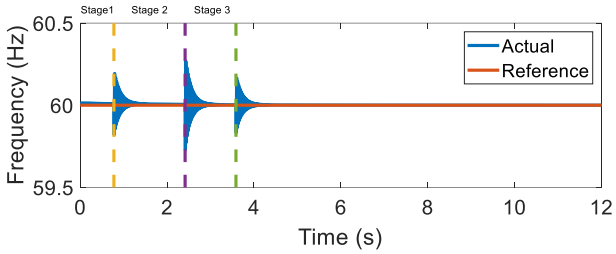

(a)

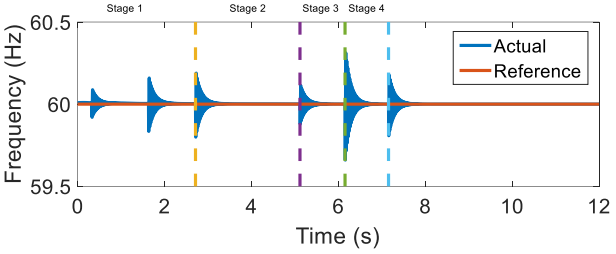

(b)

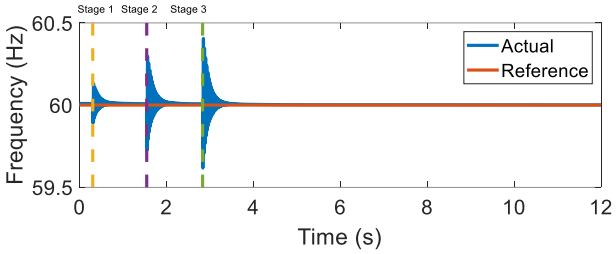

(c)

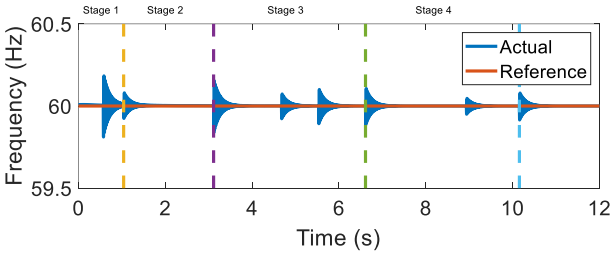

(d)

Figure 5: Frequency responses of diesel generators for four stages in case 1: (a) MG1 (b) MG2 (c) MG3 (d) MG4.

V. Discussion

The transient fault records prove that the MISOCP optimization model did not capture the complete picture of the power system. It was incapable of forecasting the transient response of generators. As a result, the optimized restoration solution resulted in severe voltage, current, and frequency spikes. These transients can damage sensitive electronic equipment and trigger the electrical protection system.

Microgrid controllers used the measurements of distributed IEDs to quantify the damage afflicted on the generators. This transient response provided feedback for the next stage of the rolling horizon optimization. In effect, the dynamic feedback based on wide-area situational monitoring improved the restoration of inverter-dominated microgrids [1] [3].

The different subsystems operated cooperatively with two-way negotiations to exchange information and control signals. Perfect coordination was required between the DERs, smart switches and microgrid controller.

VI. Conclusion

This research demonstrated a cyber-physical implementation of a resilient distribution system. The proposed decentralized restoration strategy focused on formation of microgrids. The switching sequence determined by solving the MISOCP optimization problem was implemented over a distributed multi-agent control framework. The test results have demonstrated the importance of hard real-time communication in the control and management of smart grids. Our future work on this research will focus on implementation of the MAS in a real-world application and testing the system in more complex scenarios.

VII. References

[1] Q. Zhang, Z. Ma, Y. Zhu and Z. Wang, "A two-level simulation-assisted sequential distribution system restoration model with frequency dynamics constraints", IEEE Transactions on Smart Grid, vol. 12, no. 5, pp. 3835-3846, Sept. 2021.

[2] A. Sharma, D. Srinivasan and A. Trivedi, "A decentralized multiagent system approach for service restoration using DG islanding", in IEEE Transactions on Smart Grid, vol. 6, no. 6, pp. 2784-2793, 2015.

[3] M. Ghorbani, F. Mohammadi, M. Choudhry, A. Feliachi and D. Ashby, "Hardware design for distributed MAS-based fault location in power distribution systems", 2014 IEEE PES General Meeting Conference & Exposition, pp. 1-5, 2014.

[4] A. Arif and Z. Wang, "Networked microgrids for service restoration in resilient distribution systems", in IET Generation, Transmission and Distribution, vol. 11 no. 14, pp. 3612-3619, 2017.

[5] A. Sharma, D. Srinivasan and A. Trivedi, "A decentralized multi-agent approach for service restoration in uncertain environment", in IEEE Transactions on Smart Grid, vol. 9, no. 4, pp. 3394-3405, 2018.

[6] D. Chassin, K. Schneider and C. Gerkensmeyer, "GridLAB-D: An open-source power systems modeling and simulation environment", 2008 IEEE/PES Transmission and Distribution Conference and Exposition, pp. 1-5, 2008.

[7] The NS3 network simulator. (https://www.nsnam.org).

[8] 123-Bus Feeder. [Online]. Available: https://site.ieee.org/pes-testfeeders/resources.